

Interaction between antiprotonic helium ion and He atom: Potential Energy Surface

S.N. Yudin¹, I.V. Bodrenko², and G.Ya. Korenman¹

¹*D.V.Skobeltzyn Institute of Nuclear Physics, M.V. Lomonosov Moscow State University, Moscow 119991, Russia*

E-mail: korenman@nucl-th.sinp.msu.ru

¹*Department of Physics, University of Cagliari, Cittadella Universitaria di Monserrato, S.P.8km 0.700, 09042 Monserrato, Cagliari, Italy*

Abstract

Potential Energy Surface for the $(\bar{p} - \text{He}^{2+} - \text{He})$ system is calculated in the framework of the restricted (singlet spin state) Hartree-Fock method with subsequent account of the electronic correlations within the second order perturbation method (MP2). The geometry of heavy particles is described in variables of distance r from nucleus a to antiproton, distance R from the center of mass of the $(\bar{p} - a)$ pair to He atom containing nucleus b , and an angle θ between \mathbf{r} and \mathbf{R} . The potential $V(R, r, \cos \theta)$ of the interaction between He atom and a $\bar{p} - a$ subsystem involves a total energy of two electrons in the field of three heavy particles and Coulomb interactions of the b nucleus with antiproton and the a nucleus. The expansion of this potential in terms of Legendre polynomials $P_k(\cos \theta)$ is obtained. Matrices of the multipole terms $V^k(r, R)$ ($k = 0, 1, 2$) are obtained in the basis of antiprotonic helium ion states. The results are compared with the model potential that was used earlier in the calculations of collisional Stark transitions of $(\bar{p}\text{He}^{2+})$ ion. Total cross sections of collisional Stark transitions obtained with the PES potentials exceed the model results by 15 - 20% at $E \leq 12$ K.

1 Introduction

The experimental discovery and investigation of the metastable antiprotonic states in helium have opened a new chapter in the study of antiprotonic atoms (see comprehensive reviews [1, 2]). In addition to the fundamental properties of the antiproton, these experiments give interesting insights into the interaction of antiprotonic helium with ordinary atoms and molecules. The data stimulated many theoretical papers on the mechanisms of antiprotonic helium formation, collisional quenching of the metastable states, effects of collisional (density) shift and broadening of E1-spectral lines, *etc.* The detailed study of metastable states of antiprotonic helium by the ASACUSA collaboration at the AD beam (CERN) brings further data that pose specific problems in the theory of collisional effects at low temperature (~ 10 K). Thus, the measurements of hyperfine splitting of antiprotonic

helium levels by a triple laser-microwave-laser resonance method [3, 4, 5] and their interpretation require calculations of the rates of collisional transition between HFS sublevels as well as the density shifts and broadenings of the microwave M1 spectral lines [6, 7].

Among many experimental results obtained by ASACUSA collaboration, there is one very specific: the first observation of cold long-lived antiprotonic helium ions ($\bar{p}\text{He}^{2+}$) in the states with definite quantum numbers ($n = 28 - 32$, $l = n - 1$) [8]. It was observed that these states have lifetimes $\tau \sim 100$ ns against annihilation, and rates of annihilation $\lambda = \tau^{-1}$ increased roughly as a linear function of target density at $\rho < (5 - 10) \cdot 10^{17}$ cm^{-3} and temperature $T \simeq 10$ K. The antiproton annihilation occurs in the states with small angular momentum, therefore the observed lifetime has to be attributed to the time of transitions from the initial state ($l_i \simeq 30$) to the S , P , D states. Radiative transitions from the circular orbits ($l = n - 1$) at large n are strongly suppressed, therefore a main contribution to the effective rate of annihilation comes from collisional transitions. In this case the observed values of λ (at the given ρ and T) require to have an effective cross section for the initial states $\sigma_q \sim (4 - 10) \cdot 10^{-15}$ cm^2 . This value is an order of magnitude larger than previous theoretical cross sections for collisional Stark transitions [9, 10, 11] relevant to higher kinetic energy corresponding to $T \sim 10^4$ K. In addition to huge quenching cross sections, the experiment revealed an unexpected n -dependence and isotope effect ($A = 3, 4$) for effective annihilation rates. These results also cannot be explained by earlier considerations of collisional processes of ($\bar{p}\text{He}^{2+}$).

In the papers [12, 13] collisions of cold ($\bar{p}\text{He}^{2+}$) $_{nl}$ ion with surrounding helium atoms at $T \sim 10$ K were considered in the framework of close coupling approach with account for the states with all angular momenta l from $n - 1$ to 0 at the fixed n . A model interaction between two colliding subsystems was taken as

$$V(R, r, \cos \theta) = V_0(R) + V_1(R)P_1(\cos \theta) + V_2(R)P_2(\cos \theta), \quad (1)$$

where $V_0(R)$ is an adiabatic potential of the interaction between the ionic charge (+1) and He atom, R and r are distances from the ion center of mass to He atom and from He^{2+} nucleus to \bar{p} , respectively, and θ is the angle between vectors \mathbf{R} and \mathbf{r} (see Fig.1). Second and third terms in Eq.(1) take into account interactions of electric dipole and quadrupole momenta of the ion with He atom polarized by the unit ionic charge, so

$$V_1(R) = \xi_1 r V_0'(R), \quad (2)$$

$$V_2(R) = \frac{1}{2} \xi_2 r^2 R (R^{-1} V_0'(R))', \quad (3)$$

Factors $\xi_1 = (M_A + 2m_p)/(M_A + m_p)$ and $\xi_2 = (2m_p^2 - M_A^2)/(M_A + m_p)^2$ take into account a displacement of a center of charge with respect to center of mass in the $\bar{p}A^{2+}$ system and, for ξ_2 , a difference of two masses too. A correction of order r^2 to the scalar term in (1) is omitted. The dipole and quadrupole terms in (1) can mix nl states of the ion and lead to Stark transition. Induced annihilation due to mixing with S and P states during collisions was also taken into account. The potential $V_0(R)$ is, in fact, the same as the adiabatic potential of the interaction between proton and He atom. It was approximated by the sum of the Morse potential $V_M(R)$ and the long-range polarization potential cut off

at an intermediate distance,

$$V_0(R) = V_M(R) + V_p(R), \quad (4)$$

$$V_m(R) = D_0 \{ \exp[-2\beta(R - R_e)] - 2 \exp[-\beta(R - R_e)] \}, \quad (5)$$

$$V_p(R) = -\frac{\alpha}{2R^4} \{ 1 - \exp[-\gamma(R - R_e)^4] \} \theta(R - R_e), \quad (6)$$

with the parameters[14, 15] $\alpha = 1.383$, $D_0 = 0.075$, $R_e = 1.46$, $\beta = 1.65$, $\gamma = 0.005$. Here and further in this work we use atomic units ($\hbar = e = m_e = 1$) unless otherwise specified.

This model gives cross sections of Stark transitions from circular orbits with $n \sim 30$ at $E = 10$ K that are of order or greater than effective quenching cross section σ_q . Stark transition rates averaged over thermal motion correlate similarly with the observed effective annihilation rates. Thus, the model allows to understand qualitatively the observed data. Moreover, it gives also some isotope effect with correct sign and an increasing of the rates with n . However, if to take into account a whole cascade of Stark and radiative transitions from the initial circular orbit up to annihilation from S and P states, it turns out that the obtained Stark cross sections have not enough high values.

A possible improvement of the theory can be to use an *ab initio* Potential Energy Surface (PES) for three heavy particle in the ($\bar{p} - \text{He}^{2+} - \text{He}$) system instead of the model potential (1) - (4). In this paper we calculate the potential energy surface for the mentioned system in the framework of the restricted (singlet spin state) Hartree-Fock method with subsequent account of the electronic correlations within the second order perturbation method (MP2). There are very few publications on *ab initio* PES calculations for systems involving antiproton and two or three nuclei. As far as we know, potential energy surfaces for the ($\bar{p}\text{He}^+$) - He and ($\bar{p}\text{He}^+$) - H_2 systems only were considered in the literature (see papers [16, 17] and [18], respectively). A system under consideration in this paper ($\bar{p} - \text{He}^{2+} - \text{He}$) seems to be more simple because it has only two electrons instead of three electrons in the above mentioned systems. On the other hand, our system has nonzero total charge that leads to a long-range polarization interaction between subsystem 'antiprotonic ion - He atom'. So far as we know the publications on potential energy surface for the ($\bar{p} - \text{He}^{2+} - \text{He}$) system are absent in the literature.

The paper is organized as follows. In Sec. 2 we introduce notations, outline briefly the used method of PES calculations, and define the Jacobi coordinates grid points for the calculation. The results for a general 3D view of the potential and more detailed dependencies of the PES on the variables $\cos \theta$, r and R as well as the results for calculations of the multipole expansion of interaction between atom He and a $\bar{p} - \text{He}^{2+}$ subsystem are presented in Sec. 3. Matrices of the multipole terms in the basis of ($\bar{p}\text{He}^{2+}$) $_{nl}$ states are considered and compared with the model results in Sec. 4. With these matrices we have calculated total cross sections of collisional Stark transitions. The cross sections obtained with the PES potentials exceed the model results by 15 - 20% at $E \leq 12$ K. A general conclusion is given in Sec. 5.

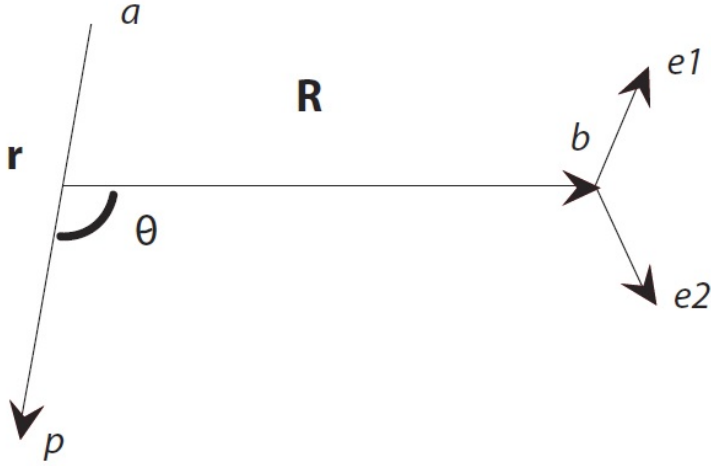


Figure 1: Jacobi coordinates of heavy particles

2 Method of calculation of the potential energy surface

The system under consideration ($\bar{p} - \text{He}^{2+} - \text{He}$) consists of two electrons and three heavy particles. Let $m_{\bar{p}}$, M_a , M_b and $\mathbf{r}_{\bar{p}}$, \mathbf{R}_a , \mathbf{R}_b be masses and coordinates of antiproton and two helium nuclei, respectively. The indexes a and b refer to the nuclei in ($\bar{p}\text{He}^{2+}$) and He atom subsystems, respectively. The c.m. coordinates of He atom coincide with the coordinates of corresponding nucleus, $\mathbf{R}_{\text{He}} \simeq \mathbf{R}_b$ with an accuracy of order m_e/M_b . The configuration of the heavy particles is defined by the Jacobi coordinates $\mathbf{r} = \mathbf{r}_{\bar{p}} - \mathbf{R}_a$ and $\mathbf{R} = \mathbf{R}_b - (\lambda\mathbf{r}_{\bar{p}} + \nu\mathbf{R}_a)$, where $\lambda = M_a/(M_a + m_{\bar{p}})$, $\nu = m_{\bar{p}}/(M_a + m_{\bar{p}})$. The heavy particles in the problem under consideration are very slow that allows to use adiabatic approximation. Then an interaction potential between two subsystem, ($\bar{p} - \text{He}^{2+}$) and He atom, can be presented as

$$V(r, R, \cos \theta) = \frac{4}{|\mathbf{R} + \nu\mathbf{r}|} - \frac{2}{|\mathbf{R} - \lambda\mathbf{r}|} + E_e(r, R, \cos \theta) - E_{\text{He}}, \quad (7)$$

where θ is the angle between the vectors \mathbf{r} and \mathbf{R} , $E_e(r, R, \cos \theta)$ is the total energy of two electrons in the field of three heavy particle (a , b and \bar{p}), and E_{He} is the ground state energy of the isolated He atom. The first two terms in (7) take into account Coulomb interaction between the ($a - \bar{p}$) subsystem and the nucleus b . Coulomb interaction between the nucleus a and antiproton ($-2/r$) is absent in (7) because it has to be included into inner energy of the ($\bar{p}\text{He}^{2+}$) ion. The potential (7) at $r \ll R$ reduces to the form of Eq. (1).

The total energy of two electrons in the field of three heavy particle $E_e(r, R, \cos \theta)$ as well as the energy E_{He} of the helium atom in the ground state were calculated in the framework of the restricted (singlet spin state) Hartree-Fock method with subsequent account of the electronic correlations within the second order perturbation method (MP2). We used the augmented correlation-consistent polarized sextuple zeta aug-cc-pV6Z and, for a comparison, quintuple zeta aug-cc-pV5Z molecular basis sets [19, 20] in the Cartesian form. The main part of the calculations involves the orbitals centered on the helium nucleus b as

well as the orbitals centered on an effective 'nucleus' with the unit positive charge placed in the ($\bar{p}\text{He}^{2+}$) center of mass. The parameters of the basis set for the latter center were taken as for hydrogen. Additional calculations with the orbitals centered only on the helium nucleus b were also done showing a reasonable results at $R \gg r$.

Parameters of the basis sets were obtained from the Extensible Computational Chemistry Environment Basis Set Database [21]. To overcome the basis set superposition error (BSSE), at every configuration, the calculations were performed with the same basis set for both the helium atom and the system of two electrons in the field of three heavy particles.

For the calculations, we used the original program taking into account a negative charge of one of heavy particles (author I.V. Bodrenko). The program employs the RI ('resolution of identity') method for the electron-electron interaction integrals and allows to perform the Hartree-Fock based calculations for large systems or for a number of configurations with moderate computational resources (see [22, 23] for details).

The potential energy was calculated at the geometry configurations corresponding to the following regular grid in the Jacobi coordinates (initial value, step, final value): $r = 0.1, 0.04, 0.9$, $R = 0.5, 0.1, 10$, $\cos \theta = -1, 0.1, +1$; totally 42336 configurations. At the each grid point the Jacobi coordinates were transformed to the Cartesian ones by using the following masses of the particles (in a.m.u.): $m_{\bar{p}} = 1.0073$; $M_{4\text{He}} = 4.0015$, $M_{3\text{He}} = 3.0149$. The calculations with two basis sets (the quintuple zeta aug-cc-pV5Z and sextuple zeta aug-cc-pV6Z) give the effectively indistinguishable values of $V(r, R, \cos \theta)$ in the mentioned region, therefore we will show below the results only for the more extended basis set (pV6Z).

3 Results for the Potential Energy Surface

A general view of the potential energy surface $V(r, R, \cos \theta)$ depending on r and R is shown in Fig. 2 for three different angles between \mathbf{r} and \mathbf{R} ($\cos \theta = +1$ corresponds to antiproton position between two nuclei). The surface is very smooth except near the points $|\mathbf{R} + \nu \mathbf{r}| = 0$ and $|\mathbf{R} - \lambda \mathbf{r}| = 0$, where one of the Coulomb terms in Eq. (7) tend to infinity.

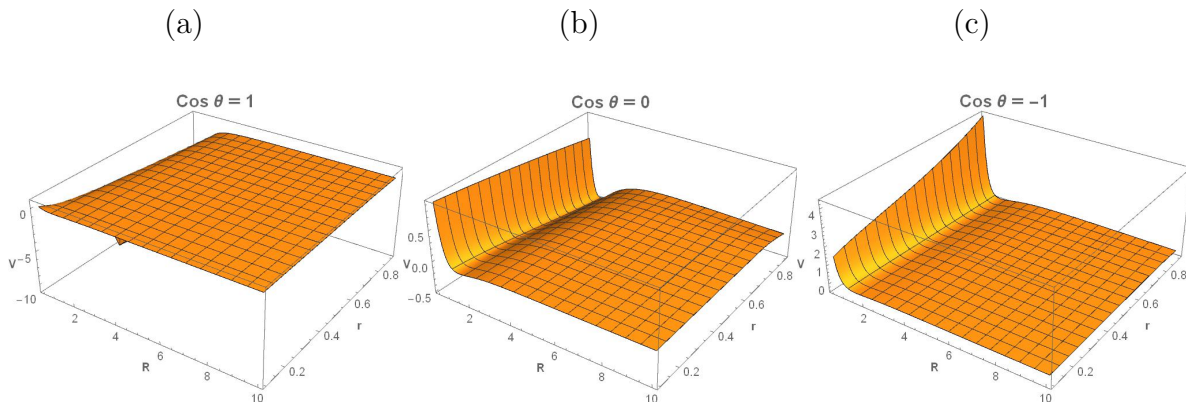


Figure 2: Potential energy surface for the system $\bar{p} - \text{He}^{2+} - \text{He}$ at (a) $\cos \theta = 1$ (antiproton between two nuclei), (b) $\cos \theta = 0$ and (c) $\cos \theta = -1$.

The potential as a function of $\cos \theta$ is shown in Fig. 3 for several values of R at $r = 0.3$ (left part of the figure), 0.5 (right part). These values of r are about the mean radii of

antiprotonic helium ion in the states $n = 30, l = n - 1$ and $l = 0$, respectively. It is seen from the Figure that a dependence of the potential on $\cos \theta$ is rather weak in the region $r \leq 0.6, R \geq 1$. Therefore the expansion of the potential energy surface in Legendre polynomials

$$V(r, R, \cos \theta) = \sum_{k=0}^{\infty} V^k(r, R) P_k(\cos \theta) \quad (8)$$

can be restricted by lowest multipoles ($k = 0, 1, 2$).

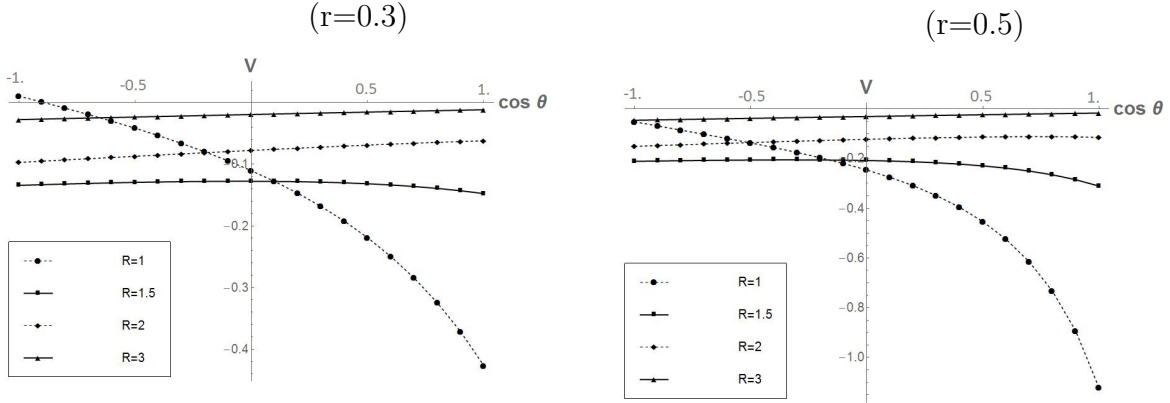


Figure 3: Dependence of PES on $\cos \theta$ for the system $\bar{p} - \text{He}^{2+} - \text{He}$ at $r = 0.3$ (left part) and $r = 0.5$ (right part) for different values of R .

Dependencies of the multipole terms $V^0(r, R)$, $V^1(r, R)$ and $V^2(r, R)$ on r and R are shown in Figs. 4 and 5. General forms of these terms are qualitatively similar to the corresponding model terms $V_0(R)$, $V_1(r, R)$ and $V_2(r, R)$, which are given by Eqs. (2) - (6). However the *ab initio* values may be quantitatively different from the model ones. It can lead to some distinctions in matrix elements (see next Section).

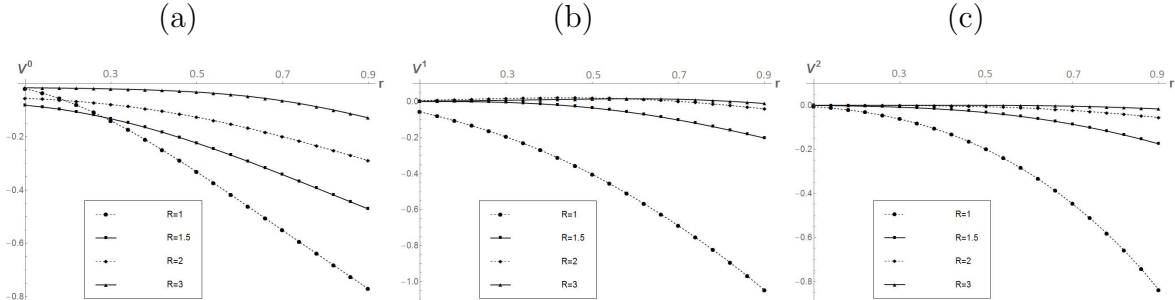


Figure 4: Dependence of scalar (a), dipole (b) and quadrupole (c) terms of the multipole expansion (8) on r at several R .

4 Matrix of the potential energy surface in the basis of antiprotonic helium ion states

Potential energy surface considered in the previous section can be used, instead of the model (1) - (6), within a quantum close-coupling approach to the collisions of ($\bar{p}\text{He}^{2+}$) ion with

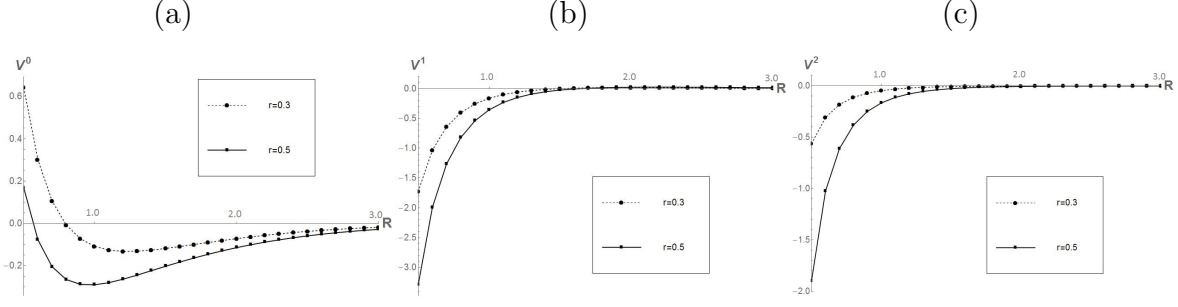


Figure 5: Dependence on R of scalar (a), dipole (b) and quadruple (c) terms of the multipole expansion (6) at $r = 0.3$ and 0.5 .

He atoms. With this in mind, we consider the potential matrix in the basis of antiprotonic helium ion wave functions

$$\langle n'l'm'|V(r, R, \cos \theta)|nlm\rangle = \delta_{ll'}\delta_{mm'}V_{nl}^0(R) + \sum_{k=1}^{\infty} V_{nl',nl}^k(R) \cdot \langle Y_{l'm'}(\Omega_r)|P_k(\cos \theta)|Y_{lm}(\Omega_r)\rangle, \quad (9)$$

where

$$V_{nl}^0(R) = V_{nl,nl}^0(R), \quad (10)$$

$$V_{nl',nl}^k(R) = \int_0^{\infty} R_{nl'}(r)V^k(r, R)R_{nl}(r)r^2dr, \quad (11)$$

$$\langle Y_{l'm'}(\Omega_r)|P_k(\cos \theta)|Y_{lm}(\Omega_r)\rangle = \langle l0k0|l'0\rangle\sqrt{4\pi/(2k+1)}\sum_q Y_{kq}^*(\Omega_R) \cdot \langle lmkq|l'm'\rangle, \quad (12)$$

$R_{nl}(r)$ are the radial hydrogen-like wave functions of antiprotonic helium ion, and $Y_{lm}(\Omega_r)$ are the ordinary spherical functions. Diagonal matrix elements (10) have the same sense as monopole term $V_0(R)$ in the model potential (1), but the formers are calculated from *ab initio* PES and depends on the $(\bar{p}\text{He}^{2+})_{nl}$ ion state. The calculated potentials $V_{nl}^0(R)$ for different n and l are shown in Fig. 6. For the comparison, the model potential $V_0(R)$ is also shown on the figure, part (a). It is seen from the figure that all calculated curves are qualitatively similar to the model potential, however they have more deep minima that are shifted to lower R as compare the R_e . Changes of $V_{nl}^0(R)$ with the quantum numbers n, l can be formulated as follows: a position of minimum shifts to lower R and a depth of minimum is increasing (a) with increasing n for circulate orbits ($l = n - 1$); (b) with decreasing of l at fixed n .

Non-diagonal matrix elements (11) at $k = 1, 2$ have to be compared with the corresponding matrix elements of the model potential. The dependencies of the model matrix elements on quantum numbers can be separated out with factors

$$I_k(nl, nl') = \langle R_{nl'}(r)|r^k|R_{nl}\rangle, \quad (13)$$

$$I_1(nl, nl - 1) = \frac{3}{2}n\sqrt{n^2 - l^2}/(\mu Z), \quad (14)$$

$$I_2(nl, nl) = \frac{1}{2}n^2[5n^2 + 1 - 3l(l + 1)]/(\mu Z)^2, \quad (15)$$

$$I_2(nl, nl - 2) = -\frac{5}{2}n^2\sqrt{(n^2 - l^2)[n^2 - (l - 1)^2]}/(\mu Z)^2. \quad (16)$$

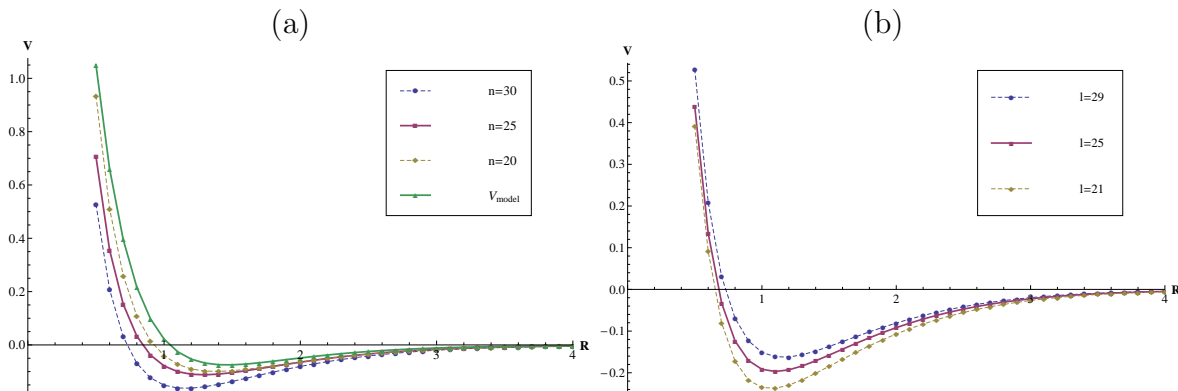


Figure 6: Dependence of $V_{nl}^0(R)$ on R (a) for circular orbits ($l = n - 1$) at different n and (b) for different l at $n = 30$. The model potential $V_0(R)$ is also shown on the part (a).

In order to exclude effects of these factors, we introduce 'scaled' matrix elements

$$\tilde{V}_{nl',nl}^k(R) = V_{nl',nl}^k(R) / (2^{-k} \xi_k I_k(nl, nl')) \quad (17)$$

that are independent on quantum numbers in the model, but can depend for the *ab initio* potentials. Radial dependencies of the dipole and quadrupole terms in the model potential (1) are defined by simple factors $V_0'(R)$ and $R(R^{-1}V_0'(R))'$ that are independent on the quantum numbers. Fig. 7 show dependencies of the 'scaled' *ab initio* dipole and quadrupole matrix elements for the circular orbits in comparison with the model. It is seen that the difference between the *ab initio* and model matrix elements is appreciable at small and intermediate R ($R \lesssim 1.5$ for $k = 1$, and $R \lesssim 2$ for $k = 2$) but it is very small at higher R .

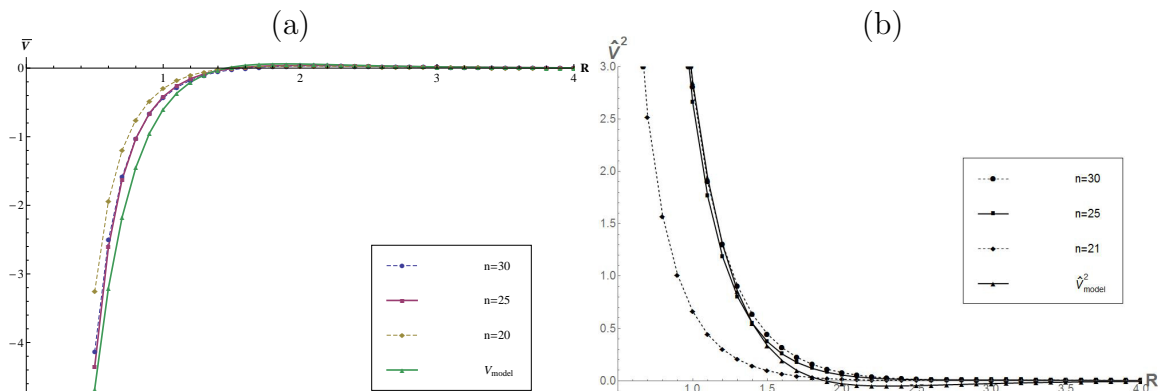


Figure 7: Dependencies of $\tilde{V}_{nn-2,nn-1}^1(R)$ and $\tilde{V}_{nn-3,nn-1}^2(R)$ on R for circular orbits at different n in comparison with the model values.

All results of the calculations shown above refer to the system with two ^4He nuclei. We have done also the same calculations for the $(\bar{p} - \text{He}^{2+} - \text{He})$ system with ^3He nuclei. Potential energy surfaces as well as the diagonal and non-diagonal matrix elements for two isotopes are very close to each other. As an example we show in Fig. 8 a comparison of monopole terms $V^0(R)$ for ^4He and ^3He at $n = 30$, $l = n - 1$ together with the model potential $V_0(R)$. It is seen that *ab initio* potentials for two isotopes are practically indistinguishable, and the both differ markedly from the model potential. It should be noted,

however, that in spite of the very close potentials, an isotope effect on dynamic characteristics (cross sections, transition rates, *etc.*) can be appreciable due the difference of the masses.

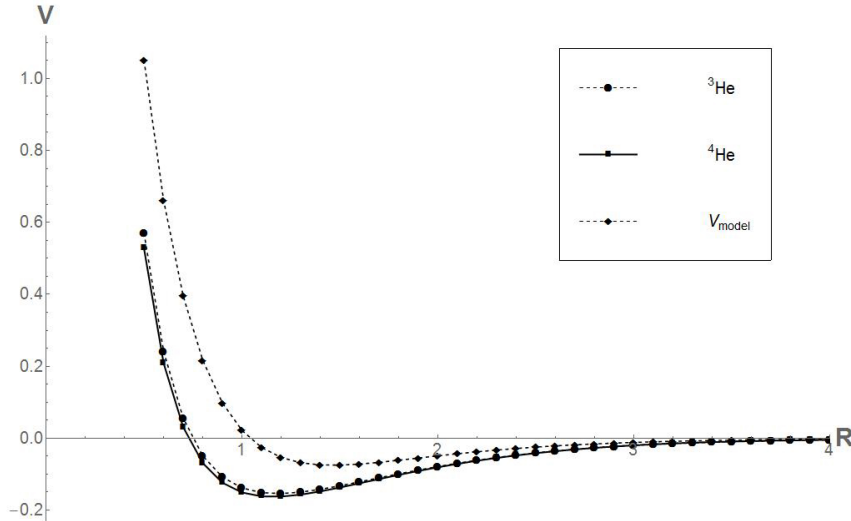


Figure 8: Monopole terms $V^0(R)$ for ${}^4\text{He}$ and ${}^3\text{He}$ at $n = 30$, $l = n - 1$ in comparison with the model potential $V_0(R)$.

We use the obtained PES potentials to calculate the cross sections of collisional Stark transition between the high states ($n \sim 30$) of ($\bar{p}\text{He}^{2+}$) ion. The calculations of Stark cross sections were done by the same close coupling method as with the model potential [12, 13]. Fig. 9 shows the results obtained with *ab initio* and model potentials for the summary cross section of Stark transition from the state $n = 30$, $l = 29$ to $l' < 29$ depending on energy. The model results contain a broad bump around 10 K that in fact is a superimposition of many resonances in different channels and partial waves [12, 13]. The cross section obtained with *ab initio* potentials has a more complicated energy dependence (two splitted bumps shifted to lower energies), because the *ab initio* potentials are deeper and depend on quantum number l of output channels. In the considered energy region ($E \leq 12$ K) the summary Stark cross section obtained with the PES potentials exceeds the model results by 15 - 20%.

5 Conclusion

We have calculated the *ab initio* potential energy surface for the ($\bar{p} - \text{He}^{2+} - \text{He}$) system in the framework of the restricted Hartree-Fock method with account of the electronic correlations within the second order perturbation method (MP2). Dependencies of the potential energy surface on R , r and $\cos \theta$ in the most interesting region are considered. At $r \leq 0.6$, $R \geq 1$ the angular dependence is rather weak that allows to use only low terms of multipole expansion. Dependencies on R and r are qualitatively similar to the model [12, 13]. Matrix of the potentials also similar to the model, however there are essential quantitative distinctions. Therefore the Stark cross sections calculated with the PES different markedly from the model. For the state $n = 30$, $l = 29$ in ($\bar{p}{}^4\text{He}^{2+}$) the

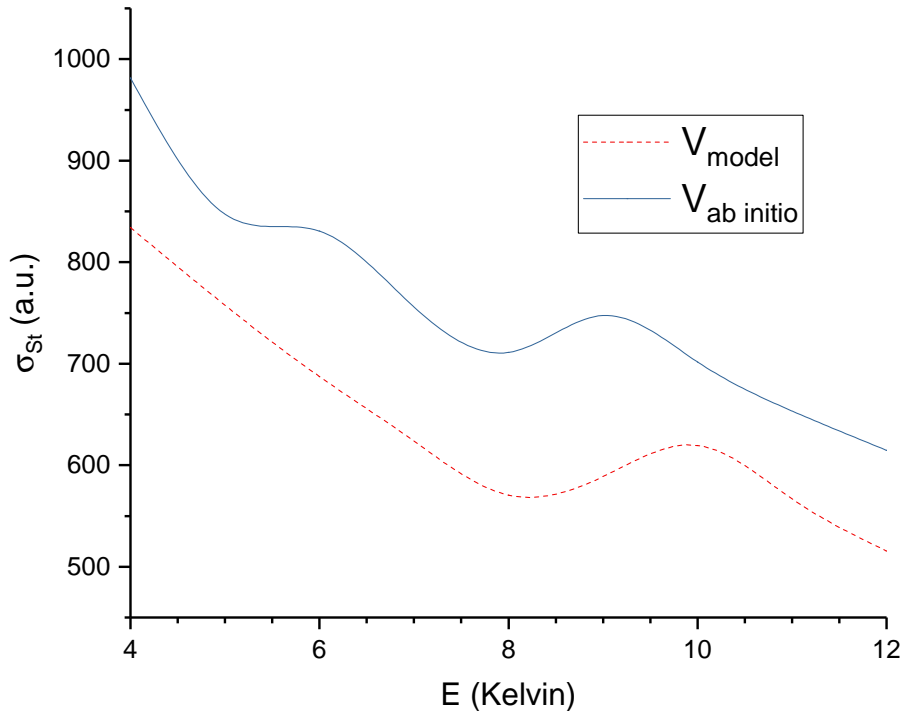


Figure 9: Summary cross sections of collisional Stark transition from $n = 30$, $l = 29$ to $l' < 29$ in $(\bar{p}^4\text{He}^{2+})$ obtained with PES and model potentials.

summary Stark cross section at $E \leq 12$ K obtained with PES potentials exceed the model results by 15 - 20%. The more detailed results for the Stark cross sections as well as for transition rates averaged over thermal motion and for the effective annihilation rates will be published separately.

Acknowledgements

One of the authors (G.K.) thanks to E.Widmann and M.Hori for the interest to our work and useful discussions.

References

- [1] T. Yamazaki, N. Morita, R.S. Hayano, E. Widmann and J. Eades, Physics Reports **366**, 183 - 329 (2002).
- [2] R.S. Hayano, M. Hori, D. Horváth and E. Widmann, Rep. Prog. Phys. **70**, 1995 - 2065 (2007).
- [3] E. Widmann, J. Eades, T. Ishikawa, *et al.*, Phys. Rev. Lett. **89**, 243402 (2002).
- [4] T. Pask, D. Barna, A. Dax, *et al.*, Phys. Letters B **678**, 55 - 59 (2009)

- [5] S. Friedreich, D. Barna, F. Caspers, *et al.*, J. Phys. B: At. Mol. Opt. Phys. **46**, 125003 (2013).
- [6] G.Ya. Korenman and S.N. Yudin, J. Phys. B: At. Mol. Opt. Phys. **39**, 1473 (2006).
- [7] S. Yudin and G. Korenman, Hyperfine Interactions **209**, 21 (2012).
- [8] M. Hori, J. Eades, R.S. Hayano, *et al.*, Phys. Rev. Lett. **94**, 063401 (2005).
- [9] G. Reifenröther, E. Klempt, and R. Landua, Phys. Lett. B **203**, 9 (1988).
- [10] R. Landua and E. Klempt, Phys. Rev. Lett. **48**, 1722 (1982).
- [11] T.S. Jensen and V.E. Markushin, Eur. Phys. J. D **19**, 165 (2002).
- [12] G.Ya. Korenman and S.N. Yudin, J. of Phys.: Conf. Series **88**, 012060 (2007).
- [13] G.Ya. Korenman and S.N. Yudin, Proc. of International Conf. on Muon Catalyzed Fusion and Related Topics (MCF-07), Dubna, JINR, 2008, p. 191-198.
- [14] J.E. Russel, Phys. Rev. A **34**, 3865 (1986).
- [15] J. Cohen, Phys. Rev. A **25**, 1791 (1982).
- [16] D. Bakalov, B. Jeziorski, T. Korona, K. Szalewicz, and E. Tchoukova, Phys. Rev. Lett. **84**, 2350 (2000).
- [17] S. Sauge, P. Valiron, Chemical Physics **265**, 47 (2001).
- [18] S. Sauge, P. Valiron, Chemical Physics **283**, 433 (2002).
- [19] T.H. Dunning, Jr., J. Chem. Phys. **90**, 1007 (1989).
- [20] D.E. Woon and T.H. Dunning, Jr. J. Chem. Phys. **100**, 2975 (1994).
- [21] Extensible Computational Chemistry Environment Basis set Database, Version 02/02/06 (EMSL), <http://www.emsl.pnl.gov/forms/basisform.html>. Current version of the database is at <https://bse.pnl.gov/bse/portal>.
- [22] A. Artemyev, A. Bibikov, V. Zayets, and I. Bodrenko, J. Chem. Phys. **123**, 024103 (2005).
- [23] A.V. Nikolaev, I.V. Bodrenko, and E.V. Tkalya, Phys. Rev. A **77**, 012503 (2008).